Steady State Temperature Profiles in Rods

Experiment No. 4

ECHE 365: Measurements Laboratory

By

Amy Chan

Submitted To:

Prof. Uziel Landau

Dept. Of Chemical Engineering

Case Western Reserve University

March 21, 2003

Group H:

Amy Chan

Anders Berliner

Catherine Chau

Erise Hosoya

Abstract

This experiment used thermocouples to measure the temperature profiles of metal rods heated by steam and cooled by either air or water. The heat transfer coefficients and thermal conductivities of the metals were also measured. Because of the additional uncertainties introduced by the rod end method and the lower percent error based on comparison with the expected h, the values calculated from the thermocouple method, where the reference positions were those of the first and last thermocouples instead of the ends of the rod, were quoted as the actual experimental values. This method gave h values of 18.8 and 9.14 W/m^2K for the air- and water-exposed methods respectively and conductivities ranging from 120 – 186 W/(m·K). The percent difference in the calculated k_{Al} values varied by about 43%, which suggested that the aluminum properties of the two rods used in this experiment could be different because of different processing or varying levels of impurities in the two rods. Fiducial marks, or the position of the origin, were concluded to shift the temperature profiles. Using a lower ΔT from the beginning of the rod to the end gives smaller values of k and h for the same amount of heat transfer. The smaller ΔT was obtained by using the first thermocouple temperature instead of the steam temperature. Comparison of the shape and values of the temperature distribution profile demonstrates that $k_{Al} > k_{steel}$. In particular, the water-cooled steel graph showed that the solution was the least accurate for the lower conductivities during simultaneous heating and cooling because of the added uncertainties. In conclusion, all of the objectives were achieved in this lab, and future studies may include testing other metals and obtaining precise positions for the ends of the rods.

Table of Contents

Objectives

This experiment was conducted to determine the temperature profiles of aluminum and steel rods that are exposed to either water or air at one end and are heated by steam at the other end. The heat transfer coefficients and thermal conductivities of aluminum were estimated from the data.

Introduction

Mechanisms of Heat Transfer

Three mechanisms exist for heat transfer: conduction, convection, and radiation. Conduction is the heat transfer though a solid or fluid, while convection is the transfer of heat between and through fluids. This report will focus on conduction and convection because radiation effects are insignificant for the given experimental conditions.

The conductive and convective heat transfer equations are defined by two different laws. Fourier's first law of heat conduction gives the amount of conduction, Q_{cond} (W), through a system. This is shown in Equation 1.

$$\vec{Q}_{cond} = -kA\nabla T \tag{1}$$

where A (m^2) is the cross sectional area, k (W/m·K) is the thermal conductivity of the material, and T (^oC) is the temperature of the material at position x (m) [1]. For conduction along one axis, Equation 1 simplifies into Equation 2.

$$Q_{cond} = -kA\frac{dT}{dx} \tag{2}$$

Newton's law of cooling gives the transfer of heat via convection, Q_{conv} (W). Equation 3 defines the convective heat transfer.

$$Q_{conv} = hS\Delta T = hS(T_s - T_a) \tag{3}$$

where the convective heat transfer coefficient is h (W/m^2K), fluid contact surface area is S (m^2), the temperature difference between the surfaces is ΔT (K), the initial reference fluid temperature is T_s (^oC), and the ambient fluid temperature is T_a (^oC) [1]. Application of Equations 2 and 3 will yield a differential energy balance for the system.

Solutions to the Energy Balance

Extended objects, such as rods or fins, are used to increase the heat transfer from the object to the surroundings. This is possible because the surface area between the solid and the ambient fluid is increased, which allows for greater convective heat transfer, as shown by Equations 2 and 3. Thus, the temperature of the rod will vary as a function of the position down its length. The rod or fin temperature distribution can be derived from an energy balance on a differential element of the object. An example is shown for the cylindrical rod in Figure 1 [1].

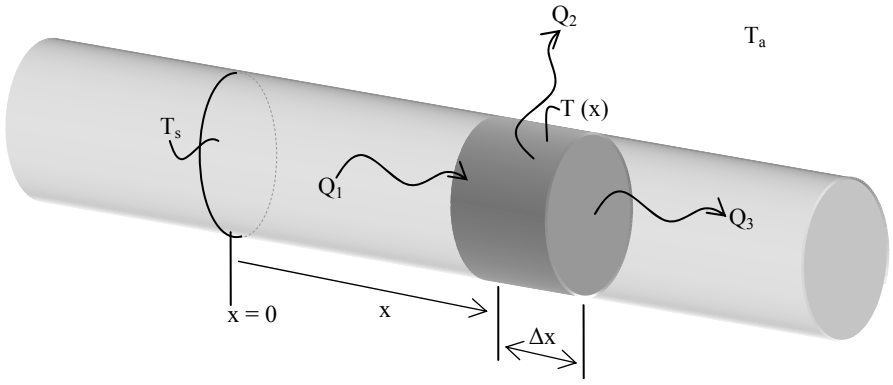

Figure 1 Energy balance for a differential element of the rod where T_s is the temperature of the rod at $x = 0$. T_a is the temperature of the surrounding fluid and Q_i represents the *i-th* element of heat transfer.

In Figure 1, Q_1 (W) and Q_3 (W) are the conduction into and out of the element respectively, while Q_3 (W) is the convective heat transfer out of the differential element to the environment. Using this nomenclature, an energy balance can be developed, as shown in Equation 4.

$$Q_1 = Q_2 + Q_3 \tag{4}$$

Substituting Equations 1 and 3 for the conductive and convective heat transfer terms of Equation 4 gives Equation 5, as shown below [1].

$$-kA\frac{dT}{dx}\bigg|_x = hS(T_s(x) - T_a) - kA\frac{dT}{dx}\bigg|_{x+\Delta x} \tag{5}$$

Rearranging Equation 5 yields Equation 6.

$$kA\frac{dT}{dx}\bigg|_{x+\Delta x} - kA\frac{dT}{dx}\bigg|_x - hS(T_s - T_a) = 0 \tag{6}$$

The equations for A and S are shown by Equations 7 and 8.

$$A = \pi \times \frac{d^2}{4} \tag{7}$$

$$S = \Delta x \times \pi \times d \tag{8}$$

where d (m) is the rod diameter. Substitution of Equations 7 and 8 into Equation 6 and dividing by Δx gives Equation 9.

$$\frac{(kA)\times\frac{dT}{dx}\bigg|_{x+\Delta x} - (kA)\times\frac{dT}{dx}\bigg|_x}{\Delta x} - hP(T_s - T_a) = 0 \tag{9}$$

where P (m)is the perimeter. Taking the limit of Equation 9 as Δx approaches zero provides Equation 10 [1].

$$\frac{d}{dx}\left((kA)\times\frac{dT}{dx}\right) - hP(T_s - T_a) = 0 \tag{10}$$

The radial temperature is assumed to be constant in the radial direction because of the following two conditions. First, this statement is true if the rod has very large aspect ratios, or the rod diameter is very small compared to the rod length. Second, the radial temperature change is negligible for rods, such as metal rods, which have high thermal conductivities. This assumption is also validated in Appendix A using the Biot Number. Therefore, the surface temperature and the temperature throughout the differential element is a constant T. This assumption yields the basic differential equation, as shown by Equation 11, for fins of uniform cross sectional area [1].

$$\frac{d^2T}{dx^2} - \frac{hP}{kA}(T - T_a) = 0 \tag{11}$$

Solutions to Equation 11 depend on the boundary conditions and have the form shown in Equation 12 and 13. Equation 13 is a rearranged version of Equation 12 [1].

$$T(x) = c_1 e^{mx} + c_2 e^{-mx} + T_a \tag{12}$$

$$T(x) = A\cosh(mx) + B\sinh(mx) + T_a \tag{13}$$

where *m* (1/m) is defined by Equation 14 [1].

$$m = \sqrt{\frac{hP}{kA}} = \sqrt{\frac{h\,\pi\,d}{k\pi\frac{d^2}{4}}} = \sqrt{\frac{4h}{kd}} \tag{14}$$

For a rod of some length, *L* (m), at a known temperature, the boundary conditions defined by Equations 15 and 16 are applicable.

$$T = T_s \qquad \text{at } x = 0 \tag{15}$$

$$T = T_L \qquad \text{at } x = L \tag{16}$$

Applying the above boundary conditions to Equation 13 provides the temperature distribution shown by Equation 17.

$$\theta = \theta_L \frac{\sinh[mx]}{\sinh[mL]} - \frac{\sinh[m(x-L)]}{\sinh[mL]} \tag{17}$$

where θ is also defined by Equation 18 [2]. The validity of this solution is shown in Appendix B.

$$\theta = \frac{T - T_a}{T_s - T_a} \tag{18}$$

More general boundary conditions, such as those in Equations 19 and 20 may also be used.

$$T = T_s \qquad \text{at } x = 0 \tag{19}$$

$$-k\frac{dT}{dx} = h(T - T_a) \qquad \text{at } x = L \tag{20}$$

Equation 20 indicates that the conduction out of the rod at its end is equal to the convection from the end of the rod to the surroundings. Applying the Equations 19 and 20 to Equation 13 provides the temperature distribution shown by Equation 21.

$$\theta = \frac{\left[\cosh[m(L-x)] + \frac{h}{mk}\sinh[m(L-x)]\right]}{\cosh[mL] + \frac{h}{mk}\sinh[mL]} \tag{21}$$

Conduction and convection both occur over the same cross sectional area at the end, so no area terms are included in Equation 21 [1]. The legitimacy of the solution shown by Equation 21 is also shown in Appendix B.

Temperatures must be known for heat transfer analysis, and many different methods exist for the measurement of temperatures. Some common temperature sensors include the thermometer, thermistor, RTD, and thermocouple. This lab will utilize thermocouples to measure the temperatures of interest. A detailed description of thermocouple theory is shown in Appendix C.

Heat Transfer Coefficients

Heat transfer coefficients can be by examining various dimensionless groups. An important group is the Nusselt number, *Nu*, which is the ratio of conductive thermal resistance to convective thermal resistance of a fluid defined by Equation 22 [1].

$$\mathrm{Nu} = \frac{\mathrm{hL_c}}{\mathrm{k_f}} \tag{22}$$

where k_f (W/mK) is the thermal conductivity of the fluid, and L_c (m) is the characteristic length of the fluid contact surface. For moving streams, *Nu* is a dependent on the Reynolds number, *Re*, and the Prandtl number, *Pr*. The Reynolds number is defined by Equation 23.

$$\mathrm{Re} = \frac{\rho \mathrm{vL_c}}{\mu} \tag{23}$$

where the fluid density is ρ (kg/m3), fluid viscosity is μ (kg/ms), and the velocity of the fluid is v (m/s). The Prandtl number is shown in Equation 24.

$$\mathrm{Pr} = \frac{\mu \mathrm{c_p}}{\mathrm{k_f}} \tag{24}$$

where c_p (J/kgK) is the heat capacity of the fluid. Because all of the dimensionless parameters (*Nu*, *Re* and *Pr*) are independent of the solid surface material properties, the heat transfer coefficient is the same for a fluid and surfaces of the same geometry but of different materials. This assumption will be used in the calculations for this experiment.

Experimental Procedure

Digital calipers made in China accurate to 0.1 mm were used to measure the diameters of the rods. The data acquisition system was a DaqBook 260, 16 bit system with expansion made by LO Tech. Furthermore, Omega thermocouples were used to record temperatures. A schematic of the system is shown in Figure 2 where the position of each thermocouple was measured using a meter stick with millimeter tick marks, labeled by a number, and recorded in Appendix D.

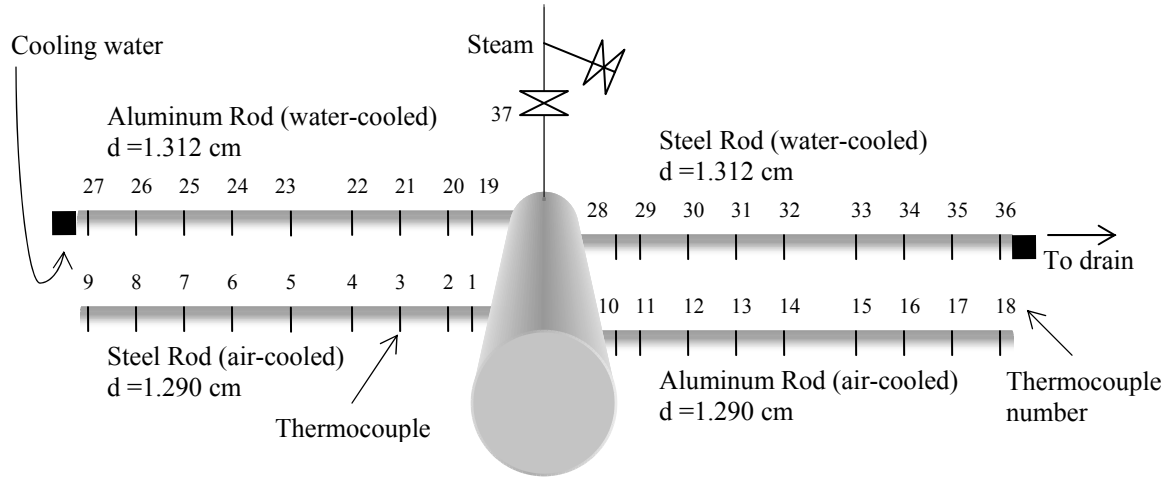

Figure 2 Labeled diagram of the experimental setup. The numbers represent the thermocouple number and the specifications of each rod are labeled accordingly.

A procedure was performed to obtain the necessary measurements. First, the data was obtained for the metal rods exposed to air on one end. The thermocouples were connected to the data acquisition system for the desired rod. The steam was started. The program was run, and temperature readings were recorded for the steam, air, water, and along the length of the rod at regular time intervals ranging from 5 to 60 seconds. When steady state was reached, at least 5 sets of steady state temperatures were recorded in 1 minute intervals. Steady state was defined as occurring when the temperature fluctuated within 0.2°C. This process of connecting the thermocouples and recording data was repeated for the second metal rod exposed to air. Because the system was at steady state from before, waiting for the second rod to achieve steady state wasn't necessary. Second, the data was obtained for the metal rods exposed to water on one end. The water was turned on and the previous procedure for the air-exposed metals was repeated for both water-exposed rods: the thermocouples were connected and the temperature readings were obtained at regular intervals and at steady state. For the second water-exposed rod, only steady state temperature readings were recorded because the system had already attained steady state during the first test.

Results and Discussion

Calculation of Conductivity and Heat Transfer Coefficients

Prior to analysis, the data columns for the thermocouples were rearranged because some of the thermocouples did not correspond to the correct zone. This was discovered after the wires were traced to the sources. The raw data is compiled in Appendix E. A plot of the temperatures down the rod during unsteady state heat transfer is shown in Figure 3 for different times.

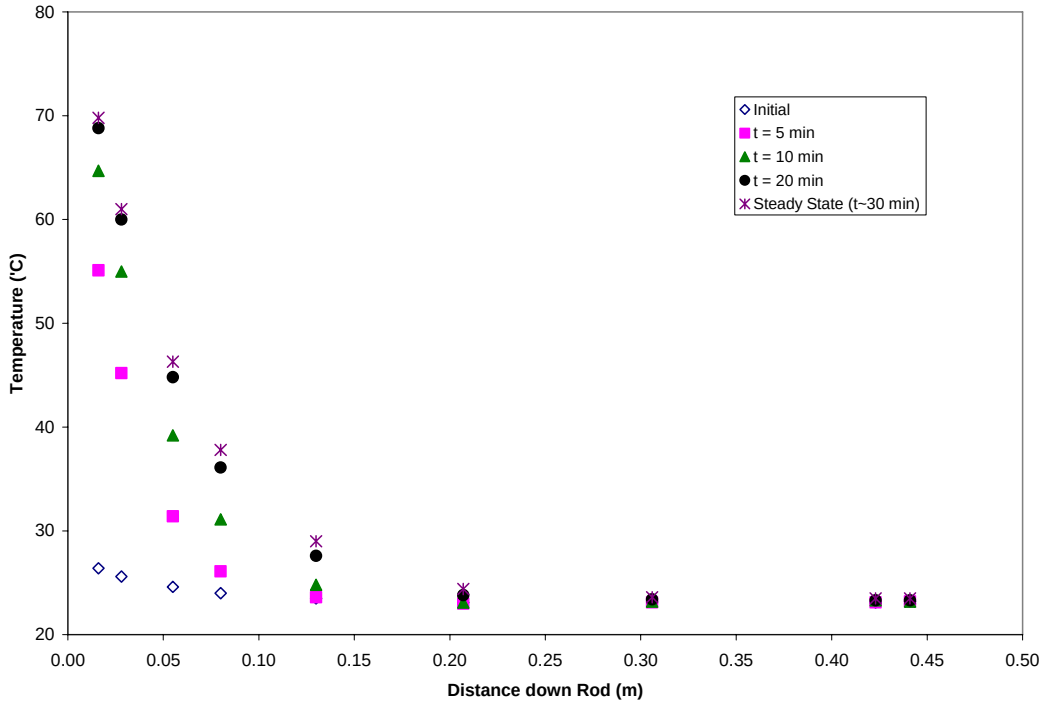

Figure 3 The temperature profile of the rod after different periods of elapsed time. The distance has the origin at the steam. The time ranged from when the steam was first turned on to when steady state was reached.

The average and standard deviations were calculated for the steady state values for all of the data sets. For the air-exposed measurements, these steady state values were used in Equations 14, 18, and 21 to obtain the values for θ as a function of h for the steel and as a function of k_{Al} for the aluminum.

$$m = \sqrt{\frac{hP}{kA}} = \sqrt{\frac{h\,\pi\,d}{k\pi\frac{d^2}{4}}} = \sqrt{\frac{4h}{kd}} \tag{14}$$

$$\theta = \frac{T - T_a}{T_s - T_a} \tag{18}$$

$$\theta = \frac{\left[\cosh[m(L-x)] + \frac{h}{mk}\sinh[m(L-x)]\right]}{\cosh[mL] + \frac{h}{mk}\sinh[mL]} \tag{21}$$

where k_{steel} was a constant 16 W/(m·K) and d was assumed to be a constant 1.3 cm for all of the calculations [1]. For the water exposed sets of data, Equation 17 replaced Equation 21, while the others remained the same.

$$\theta = \theta_L \frac{\sinh[mx]}{\sinh[mL]} - \frac{\sinh[m(x-L)]}{\sinh[mL]} \tag{17}$$

Two different methods were used to calculate the values of h and k from the above equations. First, the temperature for the first thermocouple of the air-exposed steel was used as the temperatures of the steam, T_s, because the positions and temperatures were known for both thermocouples. In addition, because of Equation 20, the total bar length was used to find the theoretical θ for the exposed air measurements. Second, the data at the steam and at the end of the rod were used for the other method. For example, the water cooled calculations of the rod end method used the temperature of the water as T_L for the calculation of θ_L because of the boundary condition of Equation 16. However, the temperature of the last thermocouple was used as T_L for the calculation of θ_L for the thermocouple method. For both situations, the value of h was assumed to be independent of the material. Because the equations were applied in the same manner for all the measurements, a representative set of calculations and results for the air-exposed steel data is shown in Appendix F. All of the results are summarized in Table 1.

Table 1 Summary of Calculations of Coefficients for the Aluminum

Situation	Calculation Method			
	First and Last Thermocouple		Ends of Rods	
	h_T (W/m^{2}K)	k_T (W/(m·K))	h_R (W/m^{2}K)	k_R (W/(m·K))
Air Exposed	18.8	186	48.3	211
Water Exposed	9.14	120	83.3	313
Percent Difference	69%	43%	-53%	-39%

where the subscript T refers to calculations made using the thermocouple method and the subscript R refers to calculations made using the rod end method. The expected value of h was $h_{exp} \approx 10$ W/m^{2}K [3]. The square difference and the percent difference of the expected and the calculated h's are summarized in Table 2.

Table 2 Summary of Difference Between h_{exp} and $h_{calculated}$

Situation	Calculation Method			
	Thermocouples		Ends of Rods	
	Δh_T^2 (W/m^{2}K)	Percent Difference with Expected Value	Δh_R^2 (W/m^{2}K)	Percent Difference with Expected Value
Air Exposed	77.44	88.0%	1466.89	383.0%
Water Exposed	0.7396	8.6%	5372.89	733.0%
Average	39.09	48.3%	3419.89	558.0%

Error Analysis

An error analysis was conducted to determine the uncertainty in the value of θ. The uncertainties in measurements are summarized in Table 3.

Table 3 Uncertainties in Measurements

Measurement (Units)	Value	Uncertainty
Temperature (°C)	Varied	f(T): ~ 0.1
Length (m)	Varied	2E-3
Diameter (m)	~0.013	~ 0
Steel Thermal Conductivity (W/m·s)	16	~ 0
θ (Unitless) – Calculated in Appendix F	Varied	f(T): ~ 2E-3

The length uncertainty was estimated by looking at the divisions, or tick marks, on the measuring device. The temperature uncertainty was a function of temperature and obtained from the standard deviation calculation in Appendix F. The diameter uncertainty was estimated from the number of decimals on the calipers. The conductivity of steel was obtained from a table [2], which showed little deviation of the heat conductivity constant with respect to temperature changes of the order 10^1 °C. The analysis and determination of the uncertainty in θ was found to be a function of temperature and is performed in Appendix G. The values of Table 2 were plotted in every graph as error bars.

Temperature Distribution Profiles

The calculated values of h and k, calculated from the data of the thermocouple technique, were used to plot the theoretical and experimental temperature distribution profiles for each situation. The reason why the thermocouple method results were used to create the plots will be discussed later. The profiles of the θ used error bars from Table 2 and are shown in Figures 4 – 7.

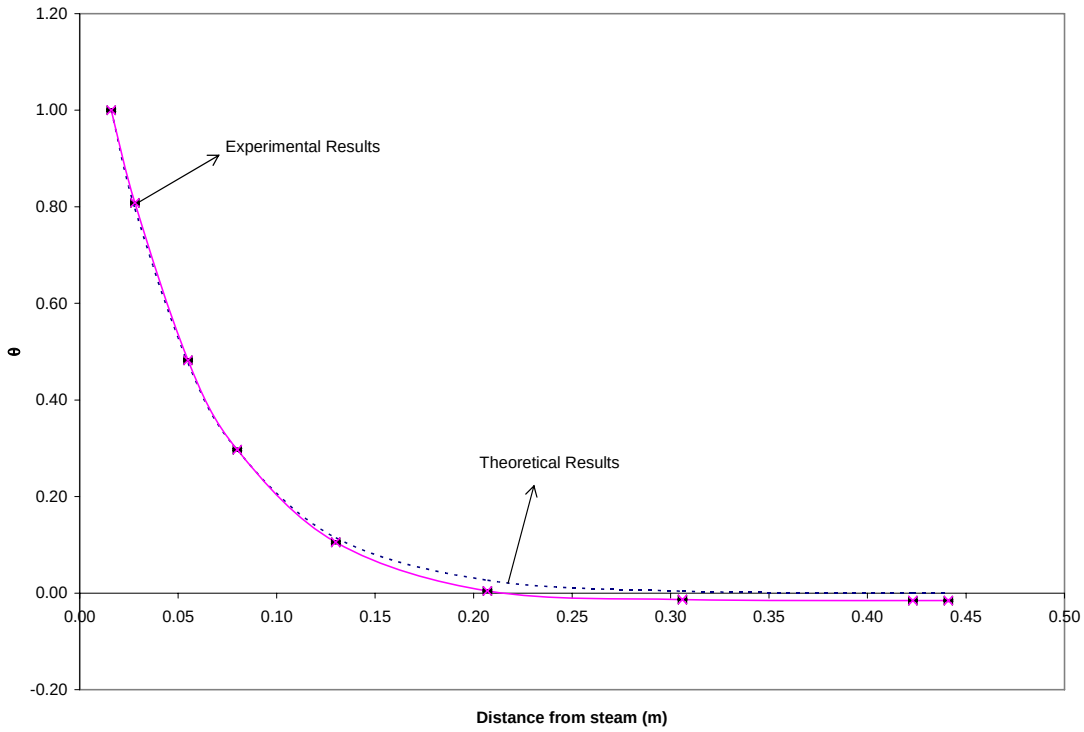

Figure 4 Temperature profile distribution for the air-cooled steel rod at steady state. The origin of this plot is the point where the rod connects with the steel canister. The experimental and theoretical θ were calculated from Equations 18 and 21 respectively.

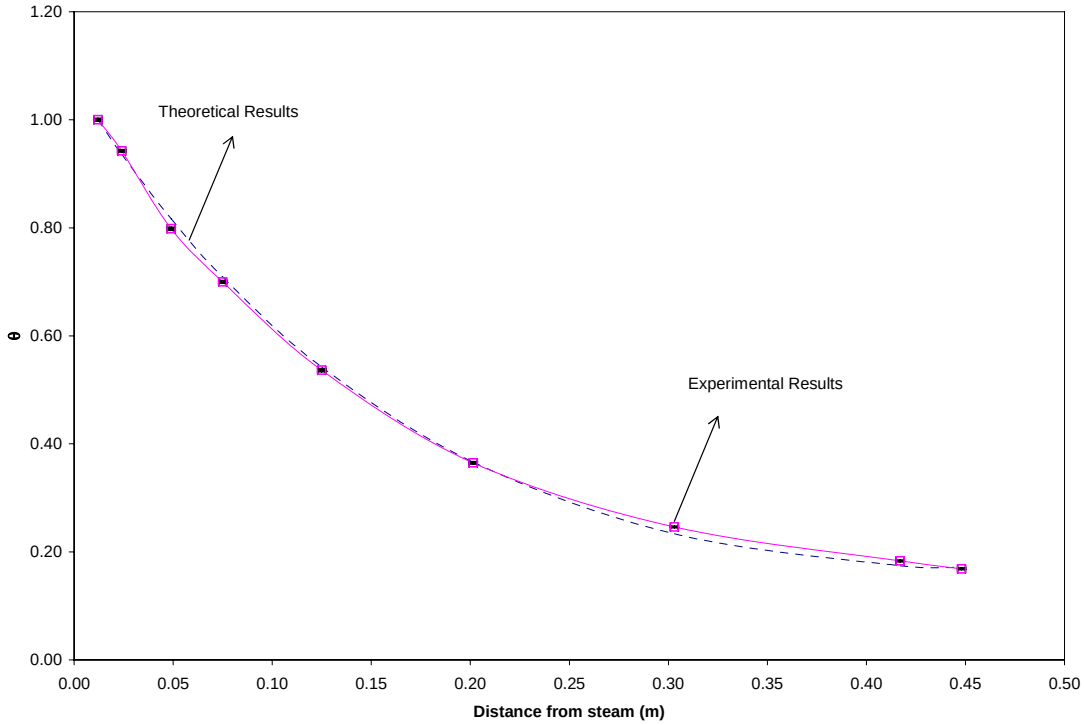

Figure 5 Temperature profile distribution for the air-cooled aluminum rod at steady state. The origin of this plot is the point where the rod connects with the steel canister. The experimental and theoretical θ were calculated from Equations 18 and 21 respectively.

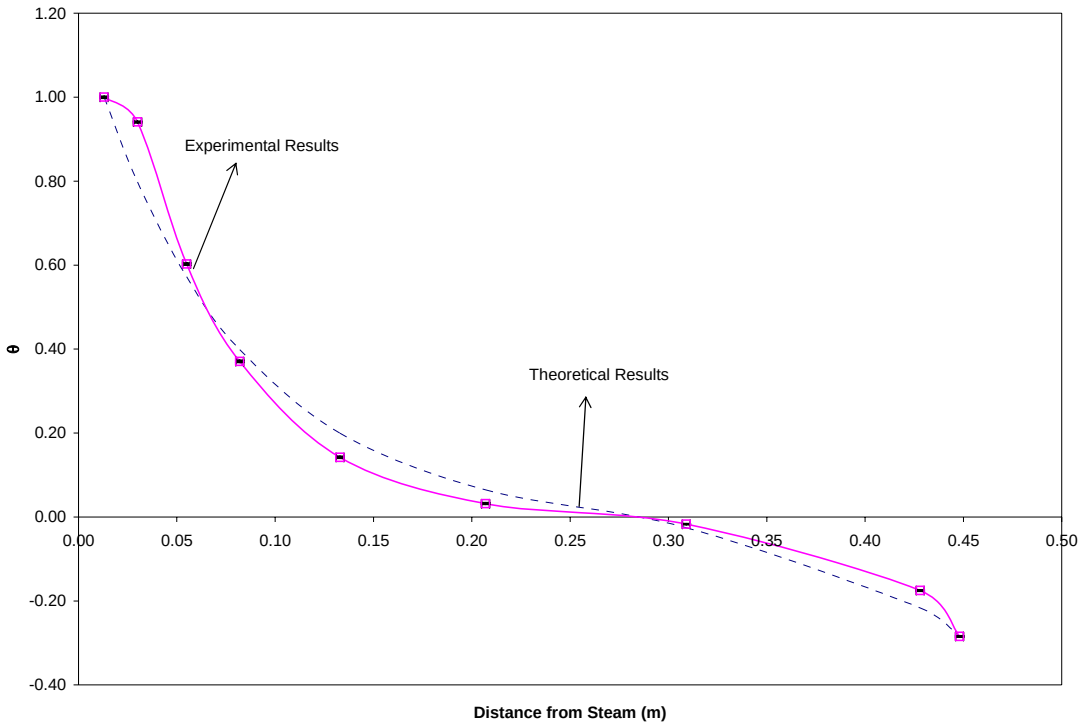

Figure 6 Temperature profile distribution for the water-cooled steel rod at steady state. The origin of this plot is the point where the rod connects with the steel canister. The experimental and theoretical θ were calculated from Equations 18 and 17 respectively.

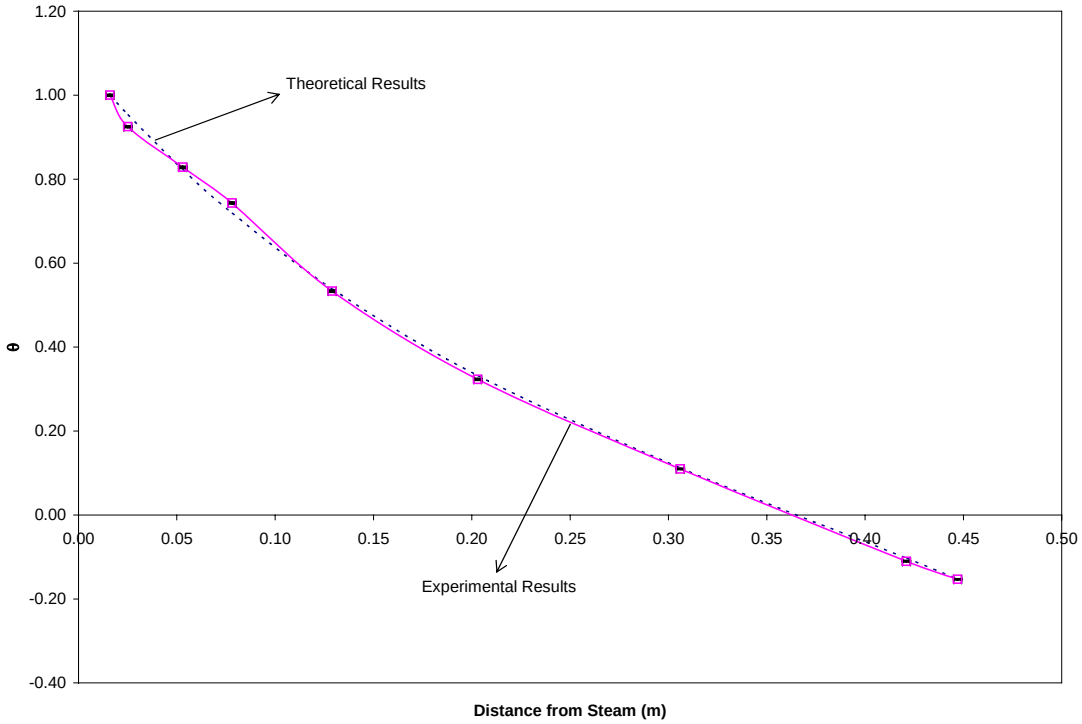

Figure 7 Temperature profile distribution for the water-cooled aluminum rod at steady state. The origin of this plot is the point where the rod connects with the steel canister. The experimental and theoretical θ were calculated from Equations 18 and 17 respectively.

Discussion of Results

Analysis of Convective and Conductive Coefficients

Depending on the calculation method, different values were obtained for h and k. The results of Table 1 showed that the thermocouple method gave h values of 18.8 and 9.14 W/m^{2}K for the air- and water-exposed methods respectively. For the end rod technique, the h values were at least 5 times greater: 48.3 and 83.3 W/m^{2}K for the air- and water-exposed methods respectively. The conductivities ranged from 120 – 186 W/(m·K) for the thermocouple method and 211 – 313 W/(m·K) for the end rod calculation method. Table 1 showed that the percent difference in the calculated k_{Al} values varied by about 43% and 39% for the thermocouple and the rod end methods respectively. Although the small difference of about 4% in the percent difference may be negligible, it does suggest that the end rod method was more accurate if the 2 values of k were supposed to the same. Thus, the values of h were compared with the expected value of 10 W/m^{2}K in Table 2, which showed that the percent error of the thermocouple method was 100 times smaller than that of the rod end method. The thermocouple method had a 48.3 percent error, while the end rod method had a 558 percent error. This difference could be due to estimations made to perform the rod end method, which introduced uncertainties that probably affected the accuracy of the calculated values. These estimations will be discussed later. Because of the fewer uncertainties and the lower percent error, the values calculated from the thermocouple method were used to create Figures 4 – 7 and will be quoted as the actual experimental values for the remaining analysis.

For the thermocouple calculated values of k, a 43 percent difference existed for the k_{Al} for the two different experimental conditions. The conductivities ranged from 120 – 186 W/(m·K), which is within the range of literature values of 120 - 226 W/(m·K) [1]. The literature values of k_{Al} varied based on the type of aluminum where pure aluminum had the higher thermal conductivities. Comparing these literature values to the thermal conductivities found in Perry's Handbook of Chemical Engineering at the same temperature gave a percent error of 18% in the theoretical values. This indicates the properties of aluminum vary widely. Thus, the aluminum properties of the two rods used in this experiment could be different, which is indicated by the different k values with percent difference of about 40%. Consequently, different processing may have occurred or varying levels of impurities existed in the two rods

Effect of Calculation Method on Coefficients

Two different methods involving different reference data were used to calculate the values of h and k in this lab. The thermocouple method used the temperatures for the first and last thermocouple of the air-exposed steel as the temperatures of the steam and rod end respectively because the positions and temperatures were known for both thermocouples. The rod end method used the data at the steam and end of the rod. The two different techniques used different fiducial marks, or different positions for the origin. For the first method, the position of the first thermocouple was subtracted from every thermocouple position to make it the origin. For the second method, the origin was the point where the rod connected with the steam container because it was assumed that the rod did not extend very far into the canister. If all of the other values, such as those of temperatures, were the same,

then the difference in fiducial marks would probably only shift the temperature profile plots. The position of the reference marks for the end points also affects the calculated values of the h and k, which will be discussed later.

The two different calculation methods provided varying levels of accuracy. Table 1 shows that the percent difference in the calculated k_{Al} values varied by about 43% and 39% for the thermocouple and the rod end methods respectively. Because the discrepancy of 4 percent difference was small, the difference in percent error of h may be compared. As mentioned earlier, Table 2 showed that the h percent error for the thermocouple method was 10^2 times smaller than that of the end rod method, which indicates a lower degree of accuracy for the end rod method. This error is a result of estimations and assumptions made during the calculations. For example, the water cooled calculations used the temperature of the water as the temperature of the end of the rod for the calculation of θ_L because of the boundary condition of Equation 16 for the rod end method of calculation. However, the length of the rod before the rod contacts water was unknown and was estimated. Furthermore, for the initial T, or T_S, the length of the rod inside the canister was assumed to be near zero. These estimations and assumptions contributed to errors because additional uncertainties were added to the system. In contrast, the thermocouple method used known temperature and positions for T_S and T_L, which made the calculations more accurate because fewer estimations were required. Thus, more accurate results are obtained when the first and the last thermocouples are used for references in the calculations because the temperatures and positions of these thermocouples are known values.

The two different techniques of calculation used in this lab also varied in the temperatures used. For the thermocouple technique, the temperature of the first thermocouple was used as the initial temperature. This temperature was lower than the steam temperature because heat was lost to the surroundings as well as down the axis of the rod. Thus, the thermocouple method used the lower ΔT from the beginning of the rod to the end because of the difference in temperatures. From Equations 2 and 3, which are the definitions of the conductive and convective heat transfers respectively, the larger ΔT will translate into higher values of k and h. This hypothesis is supported by the results of Table 1 where the thermocouple method provided h values of 18.8 and 9.14 W/m^{2}K for the air- and water-exposed methods respectively. For the end rod technique, the h values were at least 5 times greater: 48.3 and 83.3 W/m^{2}K for the air- and water-exposed methods respectively. The conductivities ranged from 120 – 186 W/(m·K) for the thermocouple method and 211 – 313 W/(m·K) for the end rod calculation method. Thus, the results showed that the h and k values calculated from the thermocouple technique were significantly less than those calculated by the end rod method. This disparity is due to the lower temperature difference between the end reference points of the thermocouple method.

Analysis of Different Temperature Distributions

The unsteady state figure from the air-exposed steel rod showed many things. First, the rate of temperature change decreased as time passed. Second, the rate of temperature change and the actual temperature change decreased as the position from the steam increased. After a certain point, negligible temperature change was observed.

Comparison of the air-cooled temperature distribution profiles demonstrates how the different k values of the metal affect the temperature along the rod. Comparing the steel temperature profiles with the aluminum profiles shows that the aluminum requires a longer distance from the heat source, which translates into higher time, to reach

the temperature of the air. Equation 18 shows that when the temperature of the rod is equal to the temperature of the air, θ is equal to 0. For the two air-cooled rods, Figure 4 shows that $\theta = 0$ when the $L \approx 0.21$ m for the steel, while Figure 5 shows that θ of the rod never equals 0 for the aluminum. The steel temperature was constant near the air temperature after 0.21 m, which infers that negligible heat was transferred after that point. From Equation 2, this shows that k_{steel} is small. The higher temperature at the end of the aluminum rod indicates greater transfer of the steam heat down the rod, which implies that $k_{Al} > k_{steel}$. Table 1 confirms this where the $k_{Al} = 153$ W/(m·K), is significantly greater than the value of $k_{steel} = 16$ W/(m·K) obtained from tables.

The shapes of the water-cooled temperature distribution profiles also give insight on the conductivity of the metals. Figures 6 and 7 show that the lengths at which $\theta = 0$ are about 0.28 m and 0.36 m for the steel and aluminum rods respectively. This difference is much smaller than the difference in lengths for the air-cooled case, which is a result of the water cooling. The lower temperature at the end of the rod creates a bigger temperature difference than for the air-cooled situation, so greater heat transfer exists because both heating and cooling are occurring simultaneously at different points of the rod. For the steel of Figure 6, the temperature begins to drop slowly near the steam vessel, but the temperature drops very quickly near the water, while a plateau is visible in the middle distances. The difference in temperature drops at the end reflects a delay in the heat transfer due to the lower k_{steel}. The plateau in the middle is near $\theta = 0$, or the temperature near the rod center is near the temperature of the air. This suggests that little heat was being transferred from the steam to the center to the water, which is expected because of the relatively low k_{steel}. Figure 7 appears very linear without a plateau, which indicates that heat was transferred constantly from the steam to the center to the water. This is expected because a higher k_{Al} translates into better heat transfer. Furthermore, because of the higher k_{Al}, the heat is being transferred immediately at the ends of the rod to prevent the curved slopes of Figure 6. In conclusion, the temperature distribution profiles support the results of $k_{Al} > k_{steel}$.

Plotting both the experimental and the theoretical θ allowed for visual comparison. First, it was noted that except for the water-cooled steel rod results shown in Figure 6, the experimental values were generally very near those of the theoretical. This indicates a high level of accuracy because the error bars were very small in each case. The water cooled steel rod showed the worst fit to the theoretical line, which may be a result of the low conductivity of steel combined with the simultaneous heating and cooling of the separate ends of the rod. The lower k translates into less heat transfer down the rod. This low heat transfer is shown when the experimental results of Figure 6 are consistently lower than the theoretical values for a range of about $0.05 < L < 0.26$ m and the rod is hotter than expected at the two rod ends. Thus, the model was not able to account for the lower conductivities during simultaneous heating and cooling because of the added complications.

Conclusions and Recommendations

The objectives of determining the temperature profiles of metal rods and estimating the heat transfer coefficients and thermal conductivities of the metals were accomplished in this lab. Depending on the calculation method, different values were obtained for h and k. The thermocouple method gave h values of 18.8 and 9.14

W/m^2K for the air- and water-exposed methods respectively. For the end rod technique, the h values were at least 5 times greater: 48.3 and 83.3 W/m^2K for the air- and water-exposed methods respectively. The conductivities ranged from 120 – 186 W/(m·K) for the thermocouple method and 211 – 313 W/(m·K) for the end rod calculation method. The percent difference in the calculated k_{Al} values varied by about 43% and 39% for the thermocouple and the rod end methods respectively, while comparing h values showed that the percent difference of the thermocouple method was 100 times smaller than that of the rod end method. The difference in h percent errors was concluded to be more significant than the difference in k percent differences, which suggested that the thermocouple method was more accurate. Because of the additional uncertainties introduced by the rod end method and the lower percent difference, the values calculated from the thermocouple method were quoted as the actual experimental values.

The thermocouple calculated conductivities ranged from 120 – 186 W/(m·K), which was within the range of literature values of 120 - 226 W/(m·K) [1]. The literature values of k_{Al} varied based on the type of aluminum where pure aluminum had the higher thermal conductivities. The high percent difference of 40% suggested that the aluminum properties of the two rods used in this experiment could be different. Consequently, different processing may have occurred or varying levels of impurities existed in the two rods.

The two different techniques used different fiducial marks, or different positions for the origin. It was hypothesized that the position of the origin, either at the intersection of the steam canister with the rod or at the first thermocouple, may not have a significant effect on the calculated values of the h and k. The two different calculation methods provided varying levels of accuracy. The estimation of the rod length before the rod contacts water and the estimation of the rod length into the steel container contributed to the inaccuracies of the calculations by introducing uncertainties. The lower accuracy of the end rod method was shown by its h percent error being 10^2 times greater than that of the thermocouple method. Thus, more accurate results are obtained when the first and the last thermocouples are used for references in the calculations because the temperatures and positions of these thermocouples are known values.

The two different techniques of calculation used in this lab also varied in the temperature difference along the rod. The thermocouple method used the lower ΔT from the beginning of the rod to the end because of the difference in the steam and first thermocouple temperatures. The smaller ΔT translated into higher values of k and h. The results stated earlier showed that the h and k values calculated from the thermocouple technique was significantly less than those calculated by the end rod method.

Comparison of the air-cooled temperature distribution profiles demonstrates how the different k values of the metal affect the temperature along the rod. For the two air-cooled rods, $\theta = 0$ when the $L \approx 0.21$ m for the steel, while the θ of the rod never equals 0 for the aluminum. For the steel, negligible temperature change occurred after $L \approx 0.21$ m because of the lower thermal conductivity. The higher temperature at the end of the aluminum rod indicates greater transfer of the steam heat down the rod, which implies that $k_{Al} > k_{steel}$. This is supported by the result of $k_{Al} = 153$ W/(m·K), which is significantly greater than the tabulated value of $k_{steel} = 16$ W/(m·K).

The shapes of the water-cooled temperature distribution profiles also imply that $k_{Al} > k_{steel}$. Greater heat transfer exists because both heating from the steam and cooling from the water are occurring simultaneously at different points of the rod. For the steel, the plateau in the middle is near $\theta = 0$, which implied that the rod center was near the temperature of the air. This suggests that little heat was transferred along the rod axis because of the

relatively low k_{steel}. The distribution for aluminum appeared linear without a plateau, which indicated that heat was transferred constantly from the steam to the center to the water. This was expected because a higher k_{Al} translates into better heat transfer to give a more linear distribution.

The accuracy of the experimental to the theoretical θ was gauged by comparing the various graphs. Except for the water-cooled steel rod results shown in Figure 6, the experimental values were generally very near those of the theoretical. This indicated a high level of accuracy because the error bars were very small in each case. The water cooled steel rod showed the worst fit to the theoretical line, which may be a result of the low conductivity of steel combined with the simultaneous heating and cooling of the separate ends of the rod. The experimental results were consistently lower than the theoretical values for a range of about $0.05 < L < 0.26$ m and the rod was hotter than expected at the two rod ends. Thus, the model was not able to account for the lower conductivities during simultaneous heating and cooling because of the added uncertainties.

Many factors can be changed for future experiments. Because the values of k were so different, additional experiments would need to be done to isolate the problem. Calculations can be made to determine a definite rod length into the canister and into the water, which will give more accurate results. In addition, different metals can be tested. The effects of unsteady state heat transfer may also be analyzed to compare the rates of heat transfer. In conclusion, many possibilities are available for further research in the field of steady state heat transfer.

Nomenclature

In Alphabetical Order:

	Symbol	Name	Units
English	A	Cross Sectional Area	m^2
	C_P	Heat Capacity	J/(kg·K)
	d	Rod Diameter	cm
	h	Convective Heat Transfer Coefficient	$W/(m^2K)$
	$h_{calculated}$	Calculated Convective Heat Transfer Coefficient	$W/(m^2K)$
	h_{exp}	Expected Convective Heat Transfer Coefficient	$W/(m^2K)$
	h_R	Convective Heat Transfer Coefficient Calculated From Rod End Method	$W/(m^2K)$
	h_T	Convective Heat Transfer Coefficient Calculated From Thermocouple Method	$W/(m^2K)$
	k	Thermal Conductivity of Metal	$W/(m^{-}K)$
	k_{Al}	Thermal Conductivity of Aluminum	$W/(m^{-}K)$
	k_f	Thermal Conductivity of Fluid	$W/(m^{-}K)$
	k_R	Thermal Conductivity Calculated from End Rod Method	$W/(m^{-}K)$
	k_{steel}	Thermal Conductivity of Steel	$W/(m^{-}K)$
	k_T	Thermal Conductivity Calculated from Thermocouple Method	$W/(m^{-}K)$
	L	Rod Length	m
	L_C	Characteristic Length	m
	m	Function Defined by Equation 14	1/m
	Nu	Nusselt Number	None
	P	Perimeter	m
	Pr	Prandtl Number	None
	Q_{cond}	Heat Transfer due to Conduction	W
	Q_{conv}	Heat Transfer due to Convection	W
	Q_i	*i*-th element of Heat Transfer	W
	Re	Reynolds Number	None
	S	Surface Area	m^2
	T	Temperature at Position *x*	°C
	T_a	Ambient Temperature	°C
	T_L	Temperature at Position *L*	°C
	T_S	Initial Reference Temperature	°C
	v	Fluid Velocity	m/s
	x	Position	m
Greek	μ	Water Viscosity	g/(m·s)
	θ	Dimensionless Temperature	None
	θ_L	Dimensionless Temperature at Position *L*	None
	ρ	Density	kg/m^3

References

1. "Fundamentals of Momentum, Heat and Mass Transfer," J. Welty, C. Wicks, R. Wilson and G. Rorrer, John Wiley & Sons, New York (2001) chapters 15, 17 and 18.
2. Private communication, Uziel Landau, Dept. of Chemical Engineering. Case Western Reserve University. Cleveland, OH.
3. Private communication, Bethany Bustard, Dept. of Chemical Engineering. Case Western Reserve University. Cleveland, OH.
4. Technical Letter. National Plastic Heater Sensor and Control Company: http://www.nphheaters.com/technical/thermo_letter.htm#thermo
5. Private communication, Craig Virnelson, Dept. of Chemical Engineering. Case Western Reserve University. Cleveland, OH.
6. Landau, Uziel. ECHE 365 – Experiment 5 Unsteady State Heat Transfer. 2003 Edition. Pg 3.

Acknowledgements

I would like to acknowledge my group members, Anders Berliner, Catherine Chau, and Erise Hosoya, for their help, advice, and dedication throughout this experiment. I would also like to thank Bethany Bustard for her guidance and patience, and Craig Virnelson for his aid during the experiment.